Photophysics of AgCl doped with $[Cl_5Ir(N\text{-methylpyrazinium})]^-$: II. ENDOR studies of ^{13}C enriched and ^{2}D exchanged complexes

2000 J. Phys.: Condens. Matter 12 2555

(http://iopscience.iop.org/0953-8984/12/11/319)

J. Phys.: Condens. Matter **12** (2000) 2555–2566. Printed in the UK PII: S0953-8984(00)08616-1

Photophysics of AgCl doped with $[Cl_5Ir(N\text{-methylpyrazinium})]^-$: II. ENDOR studies of ^{13}C enriched and ^2D exchanged complexes

Th D Pawlik, R S Eachus, R C Baetzold and W G McDugle
Imaging Materials Division, Eastman Kodak Company, Rochester, NY 14650-2021, USA

Received 7 October 1999

Abstract. Additional information has been obtained on the structure of donor complexes produced by photoelectron trapping at $[Cl_5Ir(NMP)]^-$ (NMP = N-methylpyrazinium cation) centres in AgCl microcrystals. Several different $[Cl_5Ir(NMP)]^-$ complexes were prepared by full or partial deuteration of the NMP ligand protons, and by isotopically enriching the methyl group carbon with ^{13}C. The analysis of the corresponding changes in the $[Cl_5Ir(NMP)]^{2-}$ powder ENDOR spectra made it possible to assign SHF lines to specific proton/deuteron sites. In addition, an SHF interaction from the methyl group carbon was resolved in the ^{13}C-enriched compounds. These observations, combined with preliminary results for the related donor $[(CN)_5Fe(NMP)]^{3-}$ and consideration of the *g* matrix, support the previous contention that $[Cl_5Ir(NMP)]^-$ is incorporated intact into AgCl dispersions during precipitation.

1. Introduction

In part I of this series (Eachus *et al* 2000), we presented indirect evidence that the low-spin $5d^6$ transition metal complex $[Cl_5Ir(NMP)]^-$, (NMP = N-methylpyrazinium), is incorporated intact into AgCl during precipitation from aqueous solution. Electron paramagnetic resonance (EPR) experiments have shown that its addition introduces deep electron traps, and theory predicts that a stable lattice can be achieved if this complex substitutes for $(Ag_2Cl_7)^{5-}$. In I, rather uninformative EPR spectra, that at X band consisted of single, slightly asymmetric lines with average *g* factors of about 1.97, were tentatively assigned to $[Cl_5Ir(NMP)]^{2-}$ centres associated with three or four silver ion vacancies (=V). These donors are labelled as $Ir^{\cdot}$ 3V and $Ir^{\cdot}$ 4V, respectively. However, unequivocal proof for the incorporation of this bulky complex intact has yet to be obtained.

It has been shown that electron nuclear double resonance (ENDOR) spectroscopy can provide useful information about the microscopic structure of a paramagnetic dopant complex in silver halide microcrystals when the EPR spectrum alone leaves ambiguities (Pawlik *et al* 1998, Eachus *et al* 1999). Such ambiguities are frequently due to the lack of resolved hyperfine (HF) or superhyperfine (SHF) structure. Preliminary ENDOR spectra from the $Ir^{\cdot}$ 4V centre described in I revealed SHF lines originating from hydrogen nuclei, and a comparison of the experimental results with data from theoretical calculations suggested the assignment of these lines to pyrazine ring protons. The assignment of another pair of ENDOR lines to ^{13}C interactions was considered less certain. In particular, the strong line intensity observed compared to the low natural abundance of the ^{13}C isotope (1.11%) raised serious doubts. While these ENDOR results were consistent with the organic nature of the proposed donor

0953-8984/00/112555+12$30.00

complex, it was not possible to prove directly the co-ordination of NMP to Ir in the AgCl lattice. Further data are clearly required to substantiate assignments of the EPR and ENDOR spectra to $[Cl_5Ir(NMP)]^{2-}$ centres.

In this paper, we describe two chemical approaches designed to address this issue. The first involves selective isotope substitution in the organic ligand. To this end, a number of deuterated and ^{13}C-enriched complexes have been prepared. These have been doped into AgCl dispersions and studied by EPR and ENDOR. Due to the limited availability of labelled NMP^+ cations, only a restricted set of isotope substitutions could be made.

The simultaneous resolution of HF lines from ^{191}Ir and ^{193}Ir nuclides by ENDOR would also support an assignment to $[Cl_5Ir(NMP)]^{2-}$, but this is considered unlikely in dispersions because of their small nuclear *g* factors and large quadrupole moments. The second synthetic approach we have adopted is to replace the Cl_5Ir– moiety by $(CN)_5Fe$– and to monitor the effects on the donor's magnetic resonance parameters. If they are unchanged by this substitution, then the centres assigned as $Ir^{\cdot}$ 3V and $Ir^{\cdot}$ 4V in I cannot contain $[Cl_5Ir(NMP)]^{2-}$.

2. Experiment

2.1. Materials

The dopants were prepared, purified and isolated as the salts $NMP[Cl_5Ir(NMP)]$ by the procedure described in I. For isotope substitutions, ^{13}C-enriched CH_3I and CD_3I were used to prepare the NMP cation. Pyrazine was available in its fully deuterated form, but not with ^{13}C enrichment. From these constituents five dopant complexes were synthesized with the compositions shown in table 1. These dopants, labelled (i)–(v), were structurally characterized using a combination of NMR and optical absorption spectroscopies (Toma and Malin 1973, Malin *et al* 1975, Eachus *et al* 2000). In order to investigate the possibility of proton exchange in solution, small amounts of the various deuterated samples were dissolved in H_2O and recrystallized under a nitrogen gas flow. The recrystallized materials were dissolved in D_2O and studied by proton NMR. Within the sensitivity of the NMR measurement (approximately 0.1%) there was no observable exchange. When the fully protonated sample (i) was dissolved in D_2O for NMR studies, there appeared to be no proton–deuterium exchange, even after several months at RT. There was some indication for a slow aquation step, where one of the Cl^- ligands was replaced. This rate of aquation is considered to be too slow to produce a significant amount of $[(H_2O)Cl_4Ir(NMP)]^0$ during AgX precipitation.

Cubic silver chloride microcrystals with a mean edge length of 0.35 μm were prepared as dispersions in aqueous gelatin by standard double-jet precipitation techniques (Berry 1977). They were homogeneously doped at a nominal concentration of 250 molar parts per million (mppm). A similar AgCl dispersion was prepared in which the cubic microcrystals were doped with 250 mppm of the low-spin $3d^6$ complex $[(CN)_5Fe(NMP)]^{2-}$.

For EPR and ENDOR studies, the amount of gelatin peptiser present in each sample was minimized by three aqueous dilution and centrifugation treatments (*degelling*). This procedure leaves a thin protective layer of gelatin bound to the surfaces of each AgCl microcrystal. The resultant powders were dried in air following an acetone wash, and then stored at 4 °C.

2.2. ENDOR instrumentation

ENDOR measurements were performed on a highly modified Bruker ER200D X-band spectrometer fitted with a TM_{110} mode cavity and a helium gas-flow cryostat. Optimum parameters for the ENDOR experiments were a sample temperature of 8–10 K, a microwave

Table 1. Isotopic compositions of dopants used in this study.

	Dopant	Isotope composition
(i)	$[Cl_5Ir(C_4N_2H_4CH_3)]^-$	The fully hydrogenated ligand with the methyl group carbon in natural abundance (this complex was studied in I).
(ii)	$[Cl_5Ir(C_4N_2H_4\ ^{13}CH_3)]^-$	The fully hydrogenated ligand with a ^{13}C-enriched methyl group carbon.
(iii)	$[Cl_5Ir(C_4N_2H_4\ ^{13}CD_3)]^-$	An NMP^+ ligand with a fully deuterated methyl group and a ^{13}C-enriched methyl group carbon.
(iv)	$[Cl_5Ir(C_4N_2H_4CD_3)]^-$	An NMP^+ ligand with a fully deuterated methyl group and a methyl group carbon in natural abundance.
(v)	$[Cl_5Ir(C_4N_2D_4CD_3)]^-$	The fully deuterated ligand with the methyl group carbon in natural abundance.

power of 2.5 mW at 9.44 GHz and an RF attenuation of −4 dB, with 0 dB corresponding to the full output power of a 150 W RF amplifier (Amplifier Research, 150A220A) into a 50 Ω load. The RF field was frequency modulated with a modulation depth of 350 kHz and a frequency of 1.75 kHz. The degelled AgCl dispersions were irradiated with band gap light ($\lambda = 365$ nm) to create the donor centre assigned in I as $\{[Cl_5Ir(NMP)]^{2-}.4V\}$ (=Ir· 4V), and $[(CN)_5Fe(NMP)]^{3-}.3V$ identified for the first time in this study. The irradiation temperatures were 210 and 85 K, respectively. The exposed samples were then transferred via a liquid nitrogen Dewar into the ENDOR cavity without significant warm-up.

3. Results and discussion

3.1. Isotope substitution/enrichment

The X-band (9.3 GHz) EPR spectrum assigned in I to $[Cl_5Ir(NMP)]^{2-}.4V$ (=Ir· 4V) consisted of a single, broad line ($\Delta B_{pp} \approx 4$ mT) with an averaged g factor of about 1.97. This line was slightly asymmetric, and Q-band (35 GHz) measurements revealed parallel and perpendicular g features. The ^{2}D and ^{13}C isotopic substitutions employed in this study did not manifest themselves as changes in these EPR spectra, but ENDOR measurements showed characteristic differences that clearly coincided with the substitution/enrichment of the dopant's isotopes.

Figure 1 shows X-band ENDOR spectra of AgCl dispersions doped with the five different isotopic compositions of $[Cl_5Ir(NMP)]^-$. The dopant number, as defined in table 1, is shown on the left side of each spectrum. For further clarification, the isotopic composition is shown as a formula to the right of each ENDOR spectrum. These measurements were taken at 341.5 mT, in the centre of the Ir· 4V EPR line. The first thing of note is that these powder ENDOR spectra are quite weak, despite the high doping level. For a purely isotropic SHF interaction, the ENDOR lineshape in a frequency-modulated spectrum is a symmetric derivative Lorentzian line. Most of the features in figure 1 do not have this shape, suggesting that the SHF interactions are anisotropic. In this situation, the ENDOR signals are powder patterns that generally exhibit features in the spectrum corresponding to the principal values of the SHF interaction matrix.

The nuclear g factor of deuterium is about 6.5 times smaller than that of hydrogen, and the Larmor frequency of ^{2}D is 2.23 MHz at 341.5 mT, the magnetic field chosen for the ENDOR spectra in figure 1. Since the nuclear g factor is a proportionality constant in all terms contributing to the SHF interaction (e.g., dipole–dipole interaction, Fermi contact interaction—see Spaeth *et al* 1992), the SHF interaction of ^{2}D is expected to be 6.5 times smaller than that of the proton it replaces. In addition, the deuterium nucleus has a spin of $I = 1$ and, therefore,

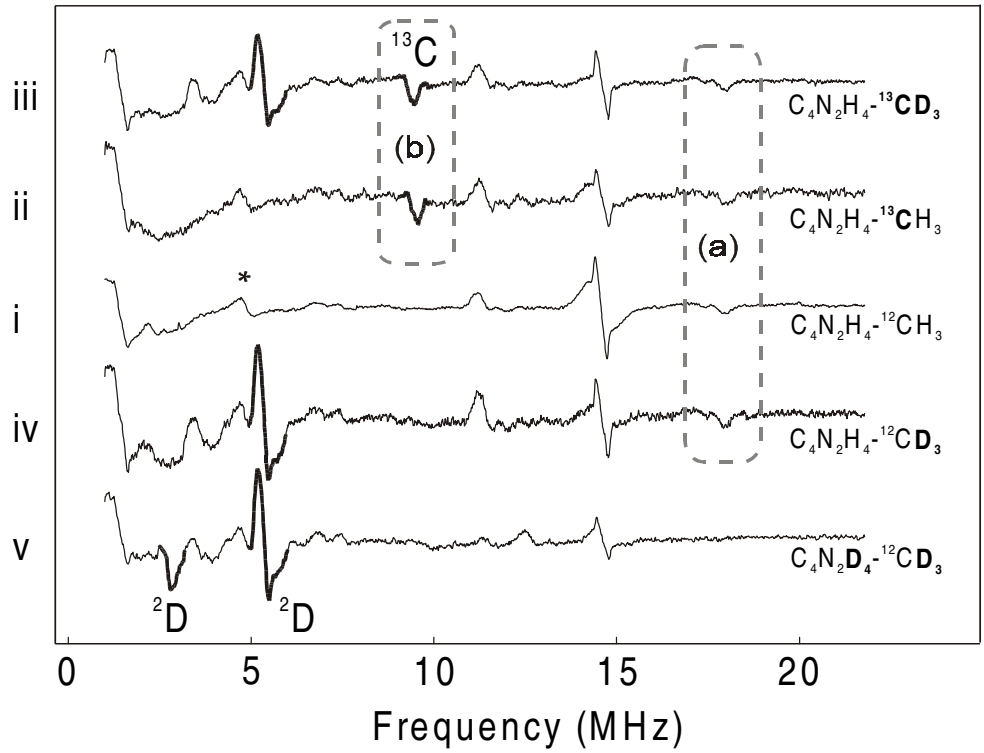

Figure 1. ENDOR spectra of dispersions with different dopant isotope compositions. The isotopic compositions of $[Cl_5Ir(NMP)]^-$ are shown to the right of each spectrum, with enrichments shown in bold fonts.

a nuclear quadrupole moment Q. The nuclear quadrupole interaction is proportional to Q and the electric field gradient at the position of the ^{2}D nucleus. In the ENDOR spectrum it can manifest itself as a splitting of the ENDOR lines into pairs with a separation proportional to the quadrupole interaction. Q for ^{2}D is quite small, roughly 1/20 that of ^{35}Cl (Weil and Rao 1997), thus a large quadrupole interaction is not expected.

The lines at 18.0 MHz and 11.2 MHz in figure 1 are assigned to hydrogen SHF interactions. They are positioned symmetrically about the Larmor frequency of ^{1}H at 14.6 MHz and correspond to ENDOR transitions in the $m_S = +1/2$ and $m_S = -1/2$ manifold of a defect with electron spin of $S = 1/2$ coupled to a proton with a nuclear spin of $I = 1/2$. From an analysis of the ENDOR lineshape, it was concluded in I that the SHF matrix was anisotropic with principal values of 6.80, 5.75 and 0 MHz. A comparison of the five spectra in figure 1 shows that the only ENDOR spectrum in which these lines do not appear (note the area marked (a)) is the spectrum from (v). Dopant (v) is the only $[Cl_5Ir(NMP)]^{2-}$ complex whose ring protons were completely replaced by deuterium. Thus, these hydrogen SHF interactions are due to ring protons, not the protons of the methyl group.

The detection of a single pair of lines from the ring protons is puzzling. Electron density at the nucleus of a ring proton results primarily from spin polarization of the >C–H σ bond. Hartree–Fock calculations performed on the optimal $(101)(\bar{1}01)(01\bar{1})(0\bar{1}\bar{1})$ geometry of Ir$^{\cdot}$ 4V predict the unpaired electron's distribution in this donor. The spin densities at C_1 and C_2 are estimated to be about twice those at C_3 and C_4 (table 2, figure 2) and, thus, two pairs of well

separated lines are expected in the ENDOR spectrum. A possible explanation for the detection of only one pair is that the missing signals are from protons H_1 and H_2 which are within 2.01 Å of N_1, the nitrogen atom carrying 66% of the unpaired electron density. Strong, anisotropic dipole–dipole interactions between the electron at N_1 and the $H_{1,2}$ nuclides might smear their ENDOR signals over a broad frequency range, precluding their detection here. While H_3 and H_4 are in equally close proximity to N_2, the spin density on this atom is only about 5%; the anisotropy resulting from dipole–dipole interactions would be correspondingly reduced. On this basis, the resolved signals from ring protons are assigned to H_3 and H_4 and correspond to spin densities on C_3 and C_4 of about 0.06 (see Atkins and Symons 1967 and I for details). This estimate is in remarkably good agreement with the Hartree–Fock value of 0.057 reported in table 2. This table also includes Hartree–Fock electron densities calculated for the most stable geometry of $Ir^{\cdot}$ 3V. Note that the unpaired electron distribution is hardly affected by the loss of the extra vacancy from $(0\bar{1}\bar{1})$. This explains why the EPR spectra of $Ir^{\cdot}$ 3V and $Ir^{\cdot}$ 4V are virtually indistinguishable (see figure 4 in I).

Table 2. Unpaired electron densities ($\times 10^3$) calculated by the Hartree–Fock method for optimum configurations of $Ir^{\cdot}$ 3V and $Ir^{\cdot}$ 4V. The latter data are taken from Eachus *et al* 1999. The indices of the nuclei are as shown in figure 2.

Vacancy configuration	Ir	$\sum$ Cl	N_1	C_1	C_2	C_3	C_4	N_2	C_5
$(101)(\bar{1}01)(0\bar{1}\bar{1})$	1.65	0.61	630.75	100.48	95.52	55.29	51.03	56.55	0.40
$(101)(\bar{1}01)(01\bar{1})(0\bar{1}\bar{1})$	1.54	0.69	661.75	82.41	79.30	57.32	57.87	51.34	0.41

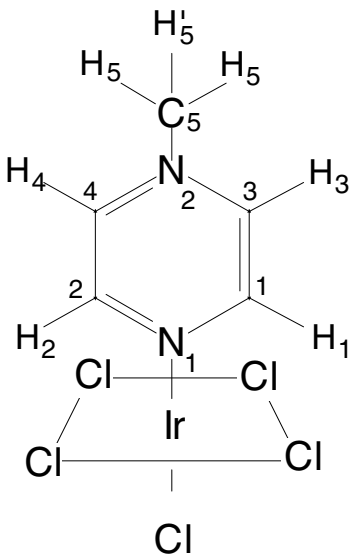

Figure 2. Schematic representation of the $[Cl_5Ir(NMP)]^{2-}$ complex. The numbers assigned to the protons as subscripts correspond to those in table 3 and Eachus *et al* (2000).

The ENDOR spectrum from (v) has a feature at 2.8 MHz (labelled (c) in figure 1) that is not present in any of the other spectra. This could originate from SHF interactions with the ring deuterium nuclei. In order to substantiate this assignment, one can scale the known ^1H SHF interaction constants with the ratio of the two nuclear g factors and simulate the ENDOR

lineshape of the ^{2}D ENDOR spectrum. The program EPR-FOR (McGavin *et al* 1993) was used for this purpose. A comparison of the measured and simulated ENDOR spectra is shown in figure 3. The right part shows the ENDOR spectrum of the fully protonated sample (i) in the frequency range of the ring proton ENDOR lines (lower trace). The upper trace is the calculated powder ENDOR spectrum using $|A_{xx}| = 6.77$ MHz, $|A_{yy}| = 5.35$ MHz and $|A_{zz}| = 0$ MHz, the parameters for the SHF matrix that gave the best fit to the experimental spectrum (table 3). These values are slightly different from those reported in I which were obtained from an ENDOR spectrum measured using amplitude modulation. The frequency modulation employed here led to improved resolution of the spectra, and, therefore, we think that the new SHF values are more accurate. Scaling with the ratio of nuclear g factors results in principal values of $|A_{xx}| = 1.04$ MHz, $|A_{yy}| = 0.82$ MHz and $|A_{zz}| = 0$ MHz for the ^{2}D SHF interaction matrix. The powder ENDOR spectrum calculated using these parameters is shown as the upper trace of the left part of figure 3. The lower trace is the experimental ENDOR spectrum of the deuterated sample (v). This comparison shows reasonable agreement between the calculated spectrum and the feature at 2.8 MHz.

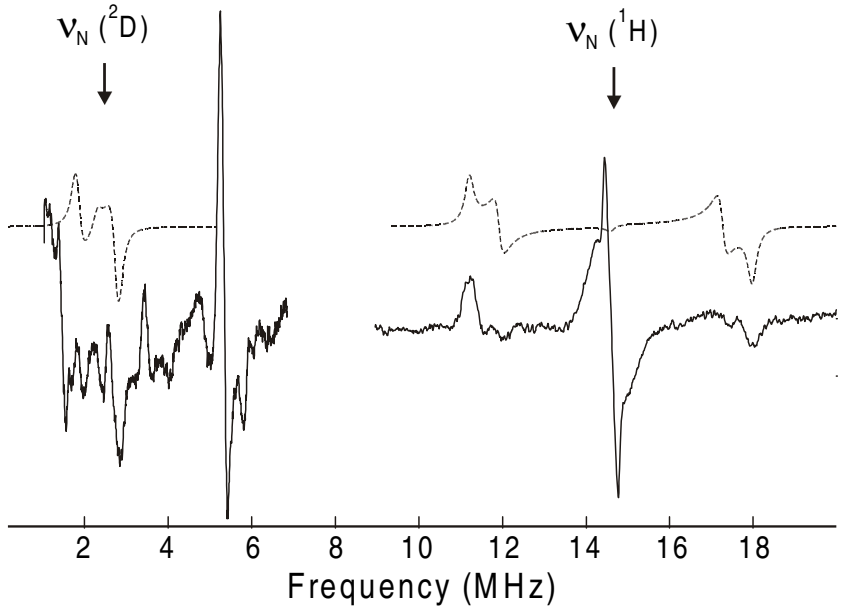

Figure 3. Right spectrum: hydrogenated $[Cl_5Ir(NMP)]^{2-}$ complex (sample (i)). Lower trace: experimental ENDOR spectrum; upper trace: ^{1}H powder spectrum calculated using $A_{xx} = 6.77$ MHz, $A_{yy} = 5.35$ MHz, $A_{zz} = 0$ MHz. Left spectrum: fully deuterated $[Cl_5Ir(NMP)]^{2-}$ complex (sample (v)). Lower trace: experimental ENDOR spectrum; upper trace: calculated powder spectrum using the values for ^{1}H scaled by the ratio of nuclear g factors for ^{2}D and ^{1}H.

A strong derivative-shaped line at 5.35 MHz and a weaker absorption-shaped line at 3.42 MHz, both labelled (d) in figure 1, are common to the ENDOR spectra of samples (iii), (iv) and (v). These samples have a deuterated methyl group in common. These ENDOR line positions correspond to deuterium SHF interactions of 6.24 MHz and 2.38 MHz, respectively. Both lines would be assigned to the $m_S = -1/2$ manifold if the SHF interaction is assumed positive. The ENDOR lines from the $m_S = +1/2$ manifold which, in both cases, should appear around 1 MHz, were not detected. This may be due to overlap with the ^{35}Cl and ^{37}Cl matrix ENDOR signals that lie in the same frequency region. Neglecting the ^{2}D nuclear

Table 3. Hyperfine interaction constants in MHz of hydrogen and carbon nuclei of the $[Cl_5Ir(NMP)]^{2-}$ complex. The indices of the protons are as shown in figure 2.

	A_{xx} (MHz)	A_{yy} (MHz)	A_{zz} (MHz)
$H_{1,2}$	6.77 ± 0.05	5.35 ± 0.2	0 ± 0.05
H_5, H_5'	34.9 ± 0.4	34.9 ± 0.4	22.4 ± 0.4
or H_5	34.9 ± 0.4	?	?
H_5'	22.4 ± 0.4	?	?
C_5	11.6 ± 0.2	?	?

quadrupole interaction, the corresponding SHF interactions of the methyl group protons would be 40.65 MHz and 15.54 MHz, respectively. Lines resulting from these protons are expected to appear in the ENDOR spectra of samples (i) and (ii) (i.e., complexes with protonated methyl groups) at 34.9 MHz for the larger interaction and 22.35 MHz for the smaller interaction. Figure 4 shows ENDOR spectra of the same set of samples with the frequency range extended to 40 MHz. There are indeed features at 23.3 MHz and 34.6 MHz, very close in frequencies to the values calculated by scaling the deuterium SHF interactions. There are several possibilities to explain two deuterium/hydrogen ENDOR lines for one m_S manifold. The observation of one absorptive and one derivative deuterium ENDOR line suggests that these correspond to parallel and perpendicular features of the SHF matrix. Figure 5 shows a powder ENDOR simulation for this case calculated assuming $A_{\parallel} = 2.38$ MHz and $A_{\perp} = 6.24$ MHz. The comparison of the simulation (upper trace) with the experimental spectrum (lower trace) shows some differences, particularly the relative magnitudes of the positive and negative branches of the derivative feature. We feel that these differences are too large to support this model. Another possible explanation for the observation of two hydrogen/deuterium features is that the three protons/deuterons of the methyl group are not equivalent. Because the $[Cl_5Ir(NMP)]^{2-}$ complex does not possess C_3 symmetry along the –Ir–N–N–CH_3 axis, an inequality of the methyl protons/deuterons is possible. The ^1H SHF interaction associated with the methyl protons results primarily from a hyperconjugative mechanism. In effect, there is direct overlap between the electronic orbitals of –CH_3 and the p_x orbital of N_2. This leads directly to two sets of non-equivalent $^1H/^2D$ nuclei, as illustrated by the model in figure 6. The hyperconjugative mechanism can lead to substantial β proton SHF interactions (Ayscough 1967), but values in the range of 20–30 MHz seem high for an >N–CH_3 fragment where Hartree–Fock calculations predict only 5% of the unpaired electron resides on the heteroatom (table 2). The discussion above assumes that the CH_3/CD_3 group does not undergo rapid rotation about the C_3 axis at the temperature of the ENDOR measurement ($\approx$10 K). When the rotation frequency is within an order of magnitude of the difference in frequencies of the two lines (i.e. 1.9 MHz for ^2D and 12.5 MHz for ^1H), a single line at their averaged value is expected.

Isotopic enrichment of the methyl group carbon led to the appearance of a line at 9.46 MHz in the ENDOR spectra of samples (ii) and (iii) (the area in question is marked (b) in figure 1). This line position corresponds to an SHF interaction of 11.60 MHz if assigned to ^{13}C. Its non-derivative shape suggests that this SHF interaction is anisotropic. However, we cannot determine all three principal values of the ^{13}C SHF matrix because no other features due to the ^{13}C enrichment are resolved.

The line at 4.92 MHz (marked with an asterisk in figure 1) and a second line at 12.39 MHz were discussed in I, but no satisfactory assignment was made. Neither line increased in amplitude following ^{13}C enrichment of the methyl carbons and, in view of their intensity in the spectrum from sample (i), they are also unlikely to originate from ring carbon nuclides. Their assignment to Ir is considered improbable. Ir has two isotopes, both with a nuclear spin

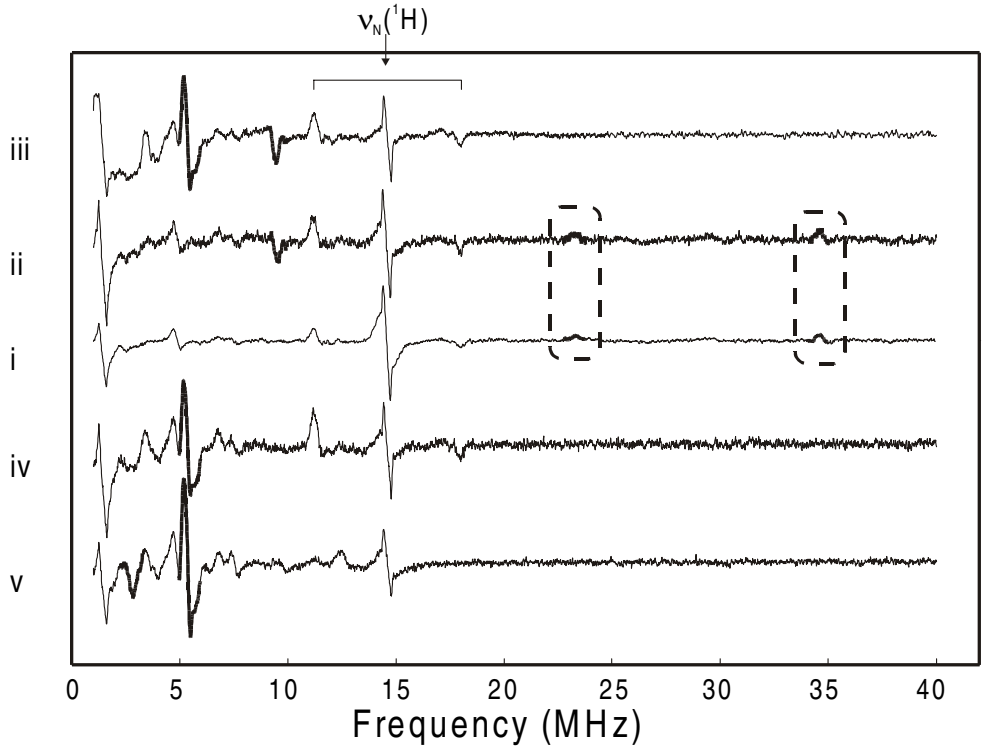

Figure 4. ENDOR spectra of $[Cl_5Ir(NMP)]^-$-doped AgCl dispersions with different isotope compositions. The sample set is the same as in figure 1. The frequency range is extended to 40 MHz.

of $I = 3/2$, with similar nuclear g factors and quadrupole moments. The ratio of ^{193}Ir:^{191}Ir in natural abundance is approximately 6:4. A quadrupole interaction will split the ENDOR transitions in each m_S state into triplets according to the selection rules $\Delta m_I = -1$, 0 and +1. The frequency position of the $\Delta m_I = 0$ transition will be least affected by the quadrupole interaction and it should give the most intense line in a powder ENDOR spectrum. Even if we assume that only the $\Delta m_I = 0$ transition is visible, we would expect to see a second line with about 60% intensity at 4.46 MHz corresponding to the less abundant ^{191}Ir nuclide. This feature was not observed. The possibility that the lines at 4.92 and 12.39 MHz are from ^{14}N was also considered in I, but discounted on the basis of field-shift experiments. Thus, we have yet to develop a satisfactory analysis of these signals.

3.2. Anisotropy of the SHF interactions

The Q-band EPR measurements described in I have clearly shown that the $[Cl_5Ir(NMP)]^{2-}$ centre has an anisotropic g matrix, as would be expected from its low symmetry. At 9.3 GHz, the difference between the field positions corresponding to $g_\parallel$ and $g_\perp$ is about 5 mT. At 35.5 GHz, this difference is almost 20 mT and it is clearly resolved as a splitting in the powder EPR spectrum. At 9.3 GHz, only a slight asymmetry in the EPR line is seen, indicating either the intrinsic EPR linewidth is large, or the EPR line is broadened because of unresolved SHF splittings. If the parallel and perpendicular features of the g matrix are well separated in the

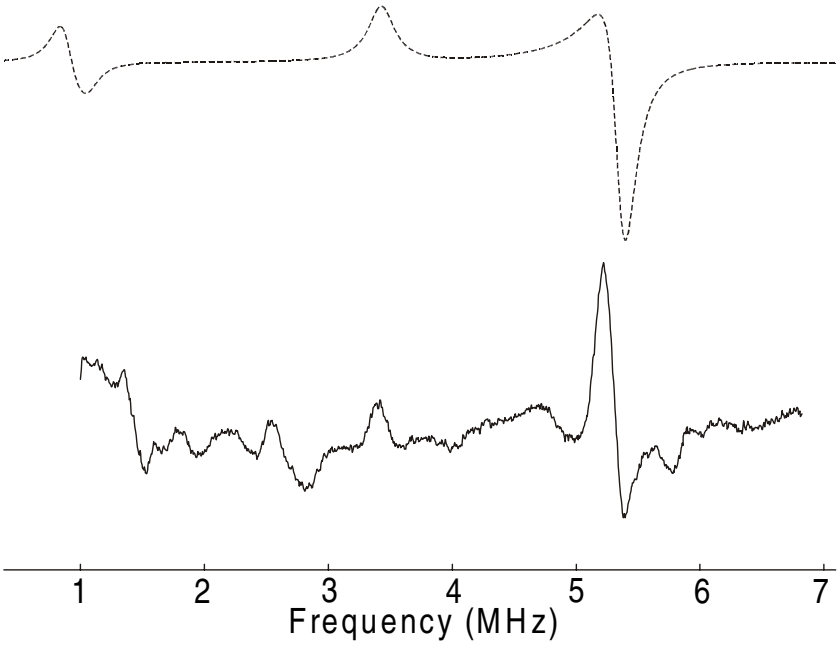

Figure 5. Experimental data (solid line) and calculated ENDOR spectrum (dotted line) of the methyl deuterium ENDOR lines under the assumption that the lines at 5.35 and 3.42 MHz are parallel and perpendicular features of a powder ENDOR spectrum.

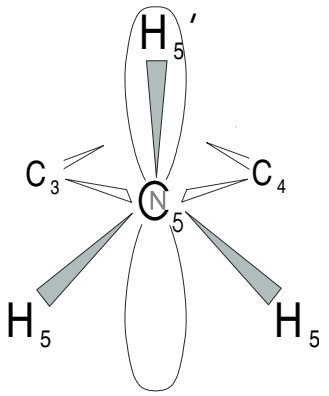

Figure 6. Model of the $>$N–CH_3 fragment in N-methylpyrazinium to illustrate the two non-equivalent β proton sites.

EPR spectrum, as is the case for donors like $[RhCl_6]^{4-}$ and $[OsCl_5(NO)]^{3-}$ in AgCl (Pawlik *et al* 1998, Eachus *et al* 1999), one can selectively excite defects whose g-matrix symmetry axes are at a specific angle to the direction of B_0, the magnetic field. If, for example, B_0 is set at a position corresponding to $g_\parallel$, the ENDOR spectrum should contain only signals from those $[Cl_5Ir(NMP)]^{2-}$ centres with their primary axis parallel to B_0. Assuming that the SHF interaction matrix of a nucleus within the complex has one axis that is collinear with $g_\parallel$ (e.g., $A_\parallel$), the ENDOR spectrum should contain signals at frequency positions corresponding

to $A_{\|}$. Figure 7(a) shows ENDOR spectra measured at various field positions within the $[Cl_5Ir(NMP)]^{2-}$ EPR line. The inset (figure 7(b)) shows the corresponding EPR spectrum with arrows indicating the field scan used in figure 7(a) and the positions corresponding to $g_{\|}$ and $g_{\perp}$. Although the anisotropy of the $[Cl_5Ir(NMP)]^{2-}$ EPR spectrum is not large enough to allow selective excitation of parallel or perpendicular centres, a scan over the magnetic field range of the EPR line should show some changes in the ENDOR spectrum. We will illustrate this for the example of the ring proton ENDOR lines whose SHF matrix was first determined by lineshape analysis in I and with greater accuracy in this paper. It was found to be anisotropic with principal values of $|A_{xx}| = 6.77$ MHz, $|A_{yy}| = 5.35$ MHz and $|A_{zz}| = 0$ MHz. The orientation of the x, y and z axes of the SHF matrix with respect to the g-matrix axes is arbitrary. Figure 7(a) shows that the ENDOR lines from these nuclei (at 11.2 MHz and 18.0 MHz) split while scanning upwards in field (i.e. from $g_{\perp}$ to $g_{\|}$). We interpret these observations in the following way: At the lowest magnetic field position (B_0 at $g_{\perp}$) the ENDOR spectrum shows features for $|A_{xx}| = 6.77$ MHz and $|A_{zz}| = 0$ MHz. When scanning upwards in field, features corresponding to $|A_{yy}| = 5.35$ MHz appear. The features corresponding to SHF values of 6.77 MHz and 5.35 MHz are visible as the splitting in the ENDOR spectrum.

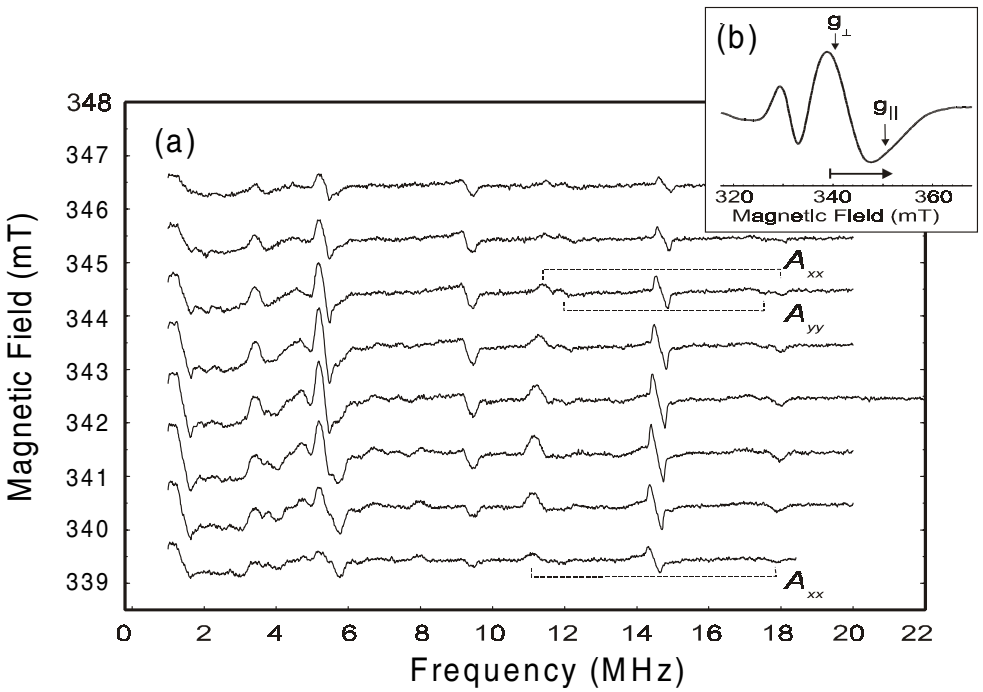

Figure 7. (a) ENDOR spectra of $[Cl_5Ir(NMP)]^{-}$-doped AgCl (sample (iii)) exposed to 365 nm light measured at different magnetic field positions, as indicated on the left-hand y axis; (b) EPR spectrum of $[Cl_5Ir(NMP)]^{-}$-doped AgCl exposed to 365 nm light. The large arrow indicates the field range covered in figure 7(a). The narrow line at about 335 mT is from a gelatin radical, $(gel)^{+}$. The positions for $g_{\|}$ and $g_{\perp}$ were calculated from Q-band data (Eachus *et al* 2000).

3.3. EPR studies of $[(CN)_5Fe(NMP)]^{2-}$*-doped AgCl*

To further substantiate our assertion that the iridium donor centres investigated in this report and I contain $[Cl_5Ir(NMP)]^{2-}$, we investigated a second set of dispersions doped with 250 mppm of the low-spin $3d^6$ complex $[(CN)_5Fe(NMP)]^{2-}$. Exposure of this degelled material to band-gap light produced high yields of the $(AgCl_6)^{4-}$ acceptor and a new paramagnetic donor. The EPR spectrum of the iron donor resembled that assigned to $[Cl_5Ir(NMP)]^{2-}$ in that it consisted of a single, slightly asymmetric line. Figure 8 compares its Q-band spectrum, measured after 365 nm irradiation at 85 K, to that assigned as $Ir^{\cdot}$ 4V. This spectrum is assigned to $[(CN)_5Fe(NMP)]^{3-}$. Changing the TM moiety from Cl_5Ir- to $(CN)_5Fe-$ has clearly effected a substantial shift to higher g factors ($g_{\|} = 1.997 \pm 0.001$, $g_{\perp} = 2.005 \pm 0.001$). A powder ENDOR spectrum obtained from $[(CN)_5Fe(NMP)]^{3-}$ also showed well resolved proton resonances. The g shifts and ENDOR data are best explained if both $[Cl_5Ir(NMP)]^{-}$ and $[(CN)_5Fe(NMP)]^{2-}$ are incorporated intact into the AgCl dispersions during precipitation.

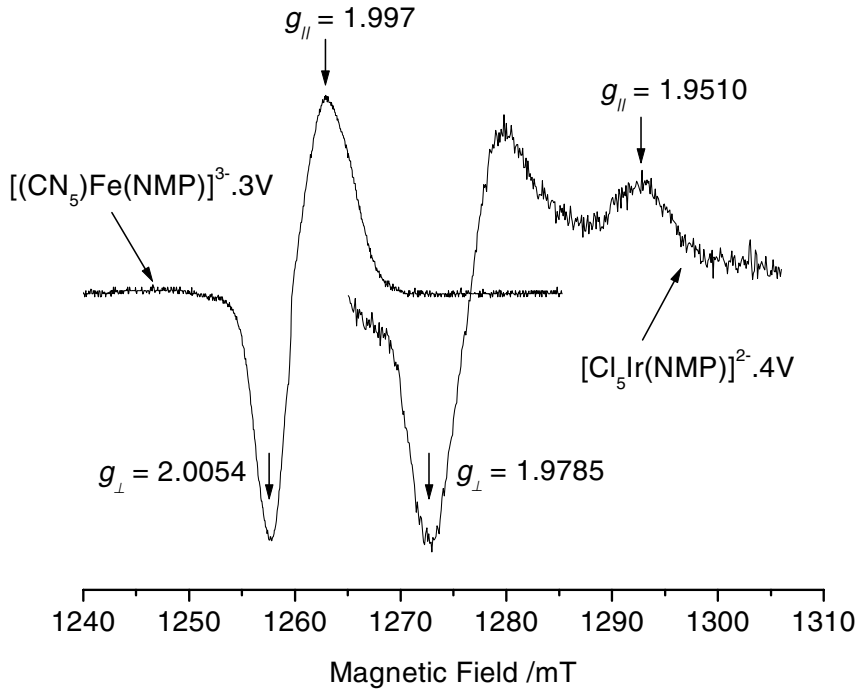

Figure 8. Q-band EPR spectra obtained at 82 K from AgCl dispersions doped with 250 mppm of $[(CN)_5Fe(NMP)]^{2-}$ or $[Cl_5Ir(NMP)]^{-}$. The spectra were obtained following 365 nm irradiation at 85 K and 210 K, respectively.

4. Summary

Through studies of a set of five AgCl dispersions containing $[Cl_5Ir(NMP)]^{-}$ with different isotopic compositions, most of the ambiguities left in I have been removed. We have shown that the proton ENDOR lines discussed in I were correctly assigned to ring protons. In addition, methyl proton and ^{13}C ENDOR lines have now been found. The assignments of the lines at 4.92 and 12.39 MHz are still incomplete, since they were not affected by the

isotope substitutions employed in this study. Our results show that the primary donor centre introduced into AgCl by addition of $[Cl_5Ir(NMP)]^-$ indeed contains the NMP moiety, and the new ENDOR measurements have given strong, albeit indirect evidence in favour of the proposed donor model. We conclude that Ir must be an integral component of the complex and some spin density must reside on this metal to account for the g shifts from 2.0023. The preliminary results reported here for the related $[(CN)_5Fe(NMP)]^{3-}$ donor in AgCl are consistent with this argument in that the proposed models of intact $[X_5M(NMP)]^{n-}$ complexes (where $M = Fe^{2+}$ or Ir^{3+}, $X = Cl^-$ or CN^-) with different spin–orbit contributions from Ir and Fe provides the most reasonable explanation for the observed g-matrix variations.

Acknowledgments

We are grateful to Professor J-M Spaeth for many helpful discussions on this work, and we wish to thank Marian Henry and Sandra Finn for preparing the silver halide dispersions used in this study.

References

Atkins P W and Symons M C R S 1967 *The Structure of Inorganic Radicals* (Amsterdam: Elsevier) ch 8
Ayscough P 1967 *Electron Spin Resonance in Chemistry* (London: Butler and Tanner) p 74
Berry C R 1977 *The Theory of the Photographic Process* ed T H James (New York: Macmillan) ch 3
Eachus R S, Baetzold R C, Pawlik Th D, Poluektov O G and Schmidt J 1999 *Phys. Rev.* B **59** 8560
Eachus R S, Pawlik Th D, Baetzold R C, Crosby D A and McDugle W G 2000 *J. Phys.: Condens. Matter* **12** 2535
Malin J M, Schmidt C F and Toma H E 1975 *Inorg. Chem.* **14** 2924
McGavin D G, Mombourquette M J and Weil J A 1993 *Computer Program EPR-FOR* version 5.1, Department of Chemistry, University of Saskatchewan
Pawlik Th D, Eachus R S, McDugle W G and Baetzold R C 1998 *J. Phys.: Condens. Matter* **10** 11 795
Spaeth J-M, Niklas J R and Bartram R H 1992 *Structural Analysis of Point Defects in Solids* (Berlin: Springer)
Toma H E and Malin J M 1973 *Inorg. Chem.* **12** 1039
Weil J A and Rao P S 1997 EPR/ENDOR frequency table *Almanac 1997* (Rheinstetten: Bruker)